Journal of Engineering and Applied Sciences 12 (Special Issue 4): 6666-6671, 2017
ISSN: 1816-949X

DIC Consistent Calibration for Indentation Mark Verification in ACF Images

[1]Bonghwan Kim, [1]Dongsu Lee, [2]Kihak Lee and [1]Kyunghan Chun
[1]Department of Electronic and Electrical Engineering, Catholic University of Daegu, Gyeongbuk, Korea
[2]R&D Center Utosys, Gyeongbuk, Korea

Abstract: The consistent calibration of DIC for indentation mark verification to ensure the electrical stability and reliability of Anisotropic Conductive Film (ACF) joints is investigated. Differential Interference Contrast (DIC) microscopy is a powerful visualization tool used to verify the indentation mark in the ACF image. It's use and setting to acquire the best image, however is not easy and not quantitative. The inherent nonlinear relationship between the object properties and the image intensity makes quantitative setting and analysis difficult. To apply consistent calibration, four calibration variables are considered and the calibration of the DIC prism slider is quantized. For the best image, the gray scale of the image is also quantized. From the test result, the proper calibration is chosen and applied.

Key words: ACF, DIC, microscopy, indentation, calibration, applied

INTRODUCTION

ACFs continue to gain popularity in the assembly of electronic devices. ACFs generally consist of adhesive resins and conductive particles and have been widely used for flip-chip applications (Watanabe *et al*., 2004). The conductive particles commonly used in ACFs are fine metal balls or metal-coated polymer balls and especially Ni/Au-coated polymer balls have been extensively used in ACFs due to their deformation and recovery behaviors during a thermo-compression bonding process (Yim *et al*., 2007). The deformation properties of the conductive particles are very important to achieve the low and stable contact resistances of ACF interconnections. Recently, some studies have been performed to understand the deformation behavior of a single conductive particle. According to the results of these studies, higher deformation degree and larger contact area of conductive particles can lead to the lower contact resistances of ACF joints. However, too high bonding force for higher deformation of conductive particles can also result in the crushing of conductive particles and the breaking of coated metal layer (Kwon and Paik, 2006; Dou *et al*., 2008). Nevertheless, in the case of ACF bonding, higher bonding force is essential to accomplish the lower contact resistances of ACF joints (Yim *et al*., 2008).

To verify the bonding of ACF, indentation mark is used and it is microscopic. For the microscopic verification, DIC microscopy is label free and is low-phototoxic, thus, it has great advantages over epifluorescence microscopy. Yet, DIC is not used for Quantitative Microscopy (QM) because the acquired images are not feasible directly for quantitative analysis. Quantitative microscopy methods such as Computational Optical Sectioning Microscopy (COSM) have been restricted to linear microscopy modalities (Erhardt *et al*., 1985). The inherent nonlinearities in the DIC image formation process have hindered past attempts at quantitative analysis.

In this study, as one of the quantitative methods for DIC calibration and ACF image verification, consistent calibration of DIC is investigated and quantized image verification is suggested. For consistent DIC calibration, four variables are considered to test and among them, DIC prism slider is only available to change and quantized by 180° and the gray scale of the result image is also quantized by picking up the maximum value of the indentation mark for quantized image verification. From the result, the best image is chosen and the consistent calibration is also accomplished. But the camera used in this study is 2 and 1-D camera is applied in factory setting. Therefore, the image verification for 1-D camera should be considered and tested in future.

DIC for indentation verification in ACF image

ACF: Flat Panel Displays (FPDs) encompass a growing number of electronic visual display technologies. Most of the modern FPDs use Liquid Crystal Displays (LCDs) technologies. ACF has been widely

Corresponding Author: Bonghwan Kim, Department of Electronic and Electrical Engineering, Catholic University of Daegu, Gyeongbuk, Korea

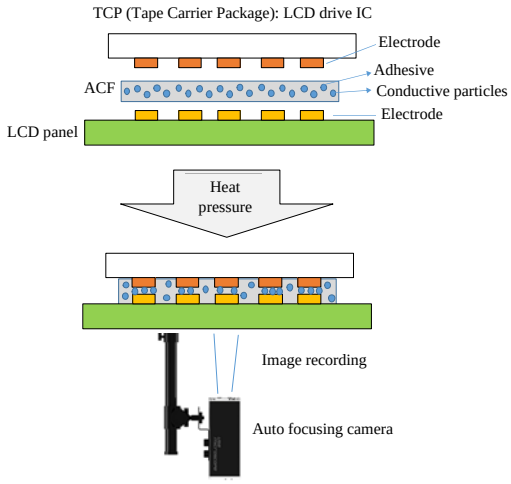

Fig. 1: Concept of ACF bonding process between TCP and LCD panel. Auto focusing camera records images and a costume-made software distinguishes between a pass and fail

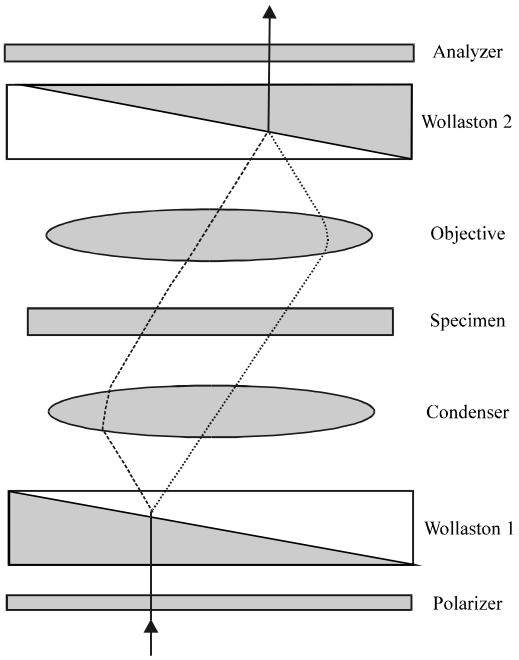

Fig. 2: Structure of DIC microscope

used in Chip on Glass (COG) bonding technology to make the electrical and mechanical connections for LCD driver IC package. Therefore, ACF is suitable to take electric interconnect between IC or flexible circuits onto various substrates like glass, organic board or flexible circuits, while it requires insulation between neighboring circuits with good adhesion. ACF technology is also used in Flex on Glass (FOG), Fglex on Board (FOB), Flex on Flex (FOF), Chip on Flex (COF), Chip on Board (COB) and similar applications for higher signal densities and smaller overall packages.

Bad bonding quality results in open or short circuits over a long bonding length between Au bump of IC chip and Indium Tin Oxide (ITO) track of glass because auto focusing indentation impression detection unit reads void-rich bonding as open circuits. Figure 1 shows the concept of ACF bonding process between Tape Carrier Packager (TCP) and LCD panel. Auto focusing camera records images and a costume-made software distinguishes between a pass and fail.

DIC: The image in a DIC microscope is formed, so that an illuminating light beam enters the microscope into a polarizer that creates plane polarized light. Then, a Wollaston prism splits the light into two mutually perpendicularly polarized light rays and a lens, called the condenser, focuses them on the specimen. The light rays pass through the specimen by a minute shear. The second lens, called the objective, transmits the lights to another Wollaston prism that recombines them. Finally, another polarizer, the analyzer transmits plane polarized light that is able to interfere and generate a contrast image (Murphy and Davidson, 2012). This setup is illustrated in Fig. 2 (Murphy and Davidson, 2012).

The Wollaston prisms and lenses are often replaced by Nomarski prisms. A Nomarski prism is technically a Wollaston prism. The difference is that its interference plane is placed from the center to a few millimeters outside of the prism. By placing the specimen in this plane the lenses become unnecessary. The arrow shows the direction of the light. The dashed and dotted lines indicate the two mutually perpendicularly polarized light rays.

The auto focusing module development for the ACF indentation test is one of the most important optical technologies. For quantitative indentation mark verification, we investigate the DIC to find which one can be calibrated. DIC is basically composed of three parts which are polarizer, analyzer and beam splitter as shown in Fig. 2. Polarizer passes only the light polarized in a specific direction. Analyzer finds out the direction of the polarization plane and the polarization amount. Nomarski prism as a beam splitter, splits the light incident on the prism into the horizontal and vertical polarized directions as shown in Fig. 3. Using these three parts, DIC microscope works as shown in Fig. 4.

At first, from the left side in Fig. 4, the light is polarized by passing through the polarizer and the Nomarski prism separates the polarized light into the horizontal and vertical polarized waves. Two waves

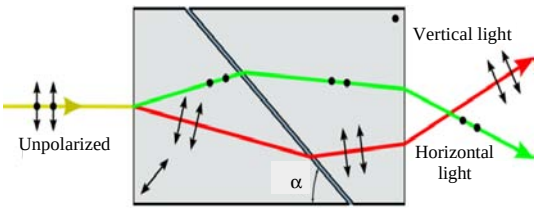

Fig. 3: Nomarski prism

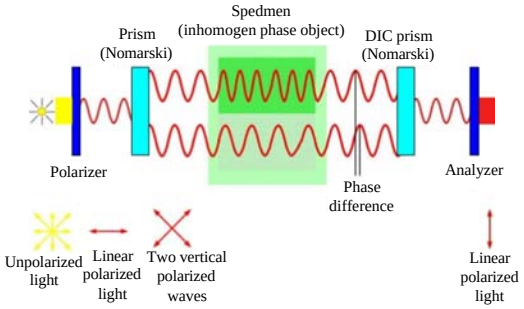

Fig. 4: DIC mechanism

become closer to tens of μm by passing through the condenser lens (experimentally 20 μm) and two lights cause a difference in their paths by reflecting or penetrating the object to observe. Passing through Nomarski prism again, two lights merge and the interference occurs in the process of merging. Using this interference pattern, we can observe the surface of the object.

MATERIALS AND METHODS

Test and validation

Test bench: For automatic ACF indentation verification, DIC microscope is installed with light source as shown in Fig. 5. GA6600 camera and Nikon TU Plan Fluor 10×0.30 lens are used. In installation, there are mark A or B on the lens case as shown in Fig. 6a and the mark A or B should be aligned with DIC prism position in Fig. 6b.

Calibration varibables: There are four adjustable parts in the test bench and they are polarizer, analyzer, light source and DIC prism. To acquire the best image in the indentation verification, these 4 parts are calibrated.

Polarizer: Among three major parts, the polarizer is mounted inside auto focus module of test bench, so, it is not adjustable.

Analyzer: Analyzer controls the light intensity by adjusting the plane angle. Although, we change slightly

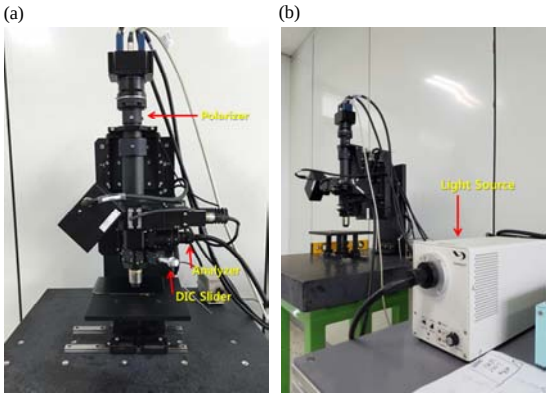

Fig. 5: a, b) Test bench

the analyzer angle, the resulting reflectance is too large because of the reflection characteristics of the LCD panel and the sensitivity of CCD sensor of the Allied Vision camera, GX-6600. So, it is difficult to obtain a clean image by calibrating the plane angle. We set the optimal angle 40° around the Z-axis and the best image is obtained in the experiment.

Light source: Light source has from 0-10 steps and step 1 and 1.5 are chosen to test by considering the sensitivity of the CCD camera because the result shows clear image at those levels. Other steps are too dark or too bright, so the indentation mark can't be verified. Two steps of light source are tested alternately at the experiment and finally step 1.5 is selected as test light source.

DIC prism: Nomarski prism is installed in the cylindrical case in Fig. 4 and 5 and adjusting the prism movement knob slides the prism up and down. Usually for DIC prism, turning the prism movement knob makes the prism do translation. But most commercial DIC slider has no gradation, so, it is not easy to calibrate consistently for the best image.

Remark: Test is accomplished for verifying the indentation mark in the image according to the slider position. We test indentation image for the knob movement from the fully close position (CW) to the fully open position (CCW) and for every 180° counterclockwise turn, the indentation image is captured and verified. This prism position is a major variable among four adjustable parts during this calibration experiment.

Quantitative calibration of DIC prism position: For numerical calibration of DIC prism position, we assume

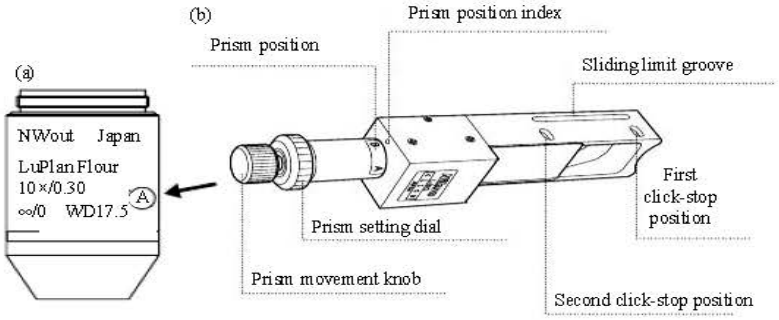

Fig. 6: a) Lense case and b) DIC prism

Fig. 7: Measurement by Vernier calipers

that the fully close position is zero and the fully open position is after nine turns CCW. And after nine turns, the maximum distance is measured as 7.1 mm (measured by Vernier calipers in Fig. 7). From the data, a turn makes the prism move by 0.789 mm because 7.1/9 turns 0.789 mm. So, we choose 0.8 mm for a turn, so 180° means 0.4 mm.

Test: For observing under the same condition, the test ACF is placed in the fixed position and only the DIC prism position is varied to verify the difference according to the change of the prism location.

For quantitative verification of indentation in ACF image, the gray scale is considered and the program to examine the gray scale of the given pixel is coded. For proper verification, the maximum gray scale value from the indentation mark is used for measurement as following:

- From ACF image, arbitrary three Tap 1-3 are selected and saved as shown in Fig. 8
- Choose three indentation marks (①, ②, ③) for each 3 Taps
- Record maximum gray scale for each chosen indentation marks

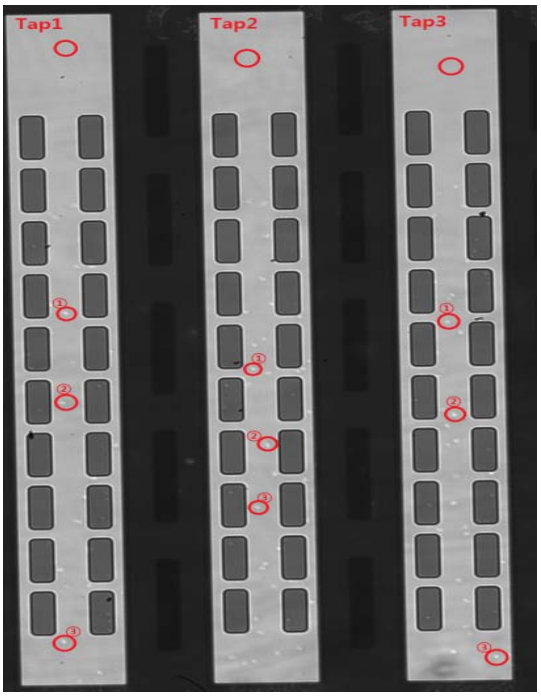

Fig. 8: Examples of gray scale measurement

RESULTS AND DISCUSSION

For the fixed panel position (polarizer, analyzer) and fixed light source step, the brightness and contrast of the acquired image is changed gradually along the DIC slider location. The brighter the image is the more visible the indentation mark is. But after some brightness, the indentation mark becomes dim again and this process is repeated cyclically.

Tap 1-3 are tested for indentation mark verification in ACF image and all show the similar variationpattern which has a period of 2.8 mm in peak value. To show exact data, Table 1, view gray scale data is attached. Therefore, we choose Tap 1 and draw a graph as shown in Fig. 9.

Table 1: Measured gray scales

Variables	1	2	3	Background
Tap 1:				
[1]-1	145.00	134.00	142.00	111.00
[1]-2	167.00	153.00	164.00	130.00
[1]-3	214.00	191.00	203.00	159.00
[1]-4	214.00	193.00	202.00	172.00
[1]-5	196.00	183.00	194.00	158.00
[1]-6	154.00	150.00	157.00	121.00
[1]-7	130.00	125.00	133.00	101.00
[1]-8	165.00	145.00	157.00	117.00
[1]-9	206.00	187.00	199.00	154.00
[1]-10	221.00	210.00	222.00	176.00
[1]-11	212.00	199.00	210.00	170.00
[1]-12	174.00	161.00	173.00	138.00
[1]-13	142.00	130.00	136.00	107.00
[1]-14	151.00	142.00	147.00	109.00
[1]-15	198.00	179.00	196.00	140.00
[1]-16	241.00	211.00	229.00	171.00
[1]-17	229.00	208.00	220.00	175.00
[1]-18	192.00	174.00	184.00	145.00
[1]-19	145.00	138.00	138.00	107.00
[1]-20	139.00	131.00	137.00	99.00
Ave	181.75	167.20	177.15	138.00
Tap 2:				
[1]-1	143.00	142.00	130.00	111.00
[1]-2	160.00	162.00	152.00	126.00
[1]-3	205.00	203.00	188.00	161.00
[1]-4	213.00	221.00	211.00	170.00
[1]-5	205.00	203.00	191.00	161.00
[1]-6	156.00	159.00	150.00	120.00
[1]-7	137.00	136.00	132.00	105.00
[1]-8	159.00	154.00	151.00	118.00
[1]-9	199.00	200.00	194.00	156.00
[1]-10	225.00	210.00	211.00	182.00
[1]-11	206.00	211.00	197.00	172.00
[1]-12	169.00	174.00	161.00	140.00
[1]-13	140.00	138.00	133.00	110.00
[1]-14	150.00	149.00	144.00	111.00
[1]-15	192.00	194.00	178.00	142.00
[1]-16	231.00	232.00	219.00	175.00
[1]-17	227.00	228.00	213.00	177.00
[1]-18	181.00	184.00	187.00	147.00
[1]-19	149.00	144.00	134.00	108.00
[1]-20	139.00	138.00	130.00	101.00
Ave	179.30	179.10	170.30	139.65
Tap 3:				
[1]-1	143.00	142.00	152.00	112.00
[1]-2	170.00	170.00	175.00	128.00
[1]-3	198.00	210.00	200.00	157.00
[1]-4	215.00	229.00	220.00	177.00
[1]-5	198.00	211.00	201.00	160.00
[1]-6	150.00	160.00	159.00	124.00
[1]-7	139.00	136.00	145.00	104.00
[1]-8	161.00	160.00	154.00	118.00
[1]-9	194.00	207.00	206.00	152.00
[1]-10	226.00	220.00	221.00	177.00
[1]-11	211.00	217.00	215.00	169.00
[1]-12	174.00	174.00	177.00	138.00
[1]-13	138.00	141.00	149.00	108.00
[1]-14	150.00	154.00	162.00	109.00
[1]-15	173.00	188.00	192.00	140.00
[1]-16	226.00	229.00	229.00	171.00
[1]-17	219.00	233.00	223.00	175.00
[1]-18	180.00	193.00	186.00	148.00
[1]-19	146.00	147.00	149.00	109.00
[1]-20	143.00	146.00	138.00	101.00
Ave	177.70	183.35	182.65	138.85

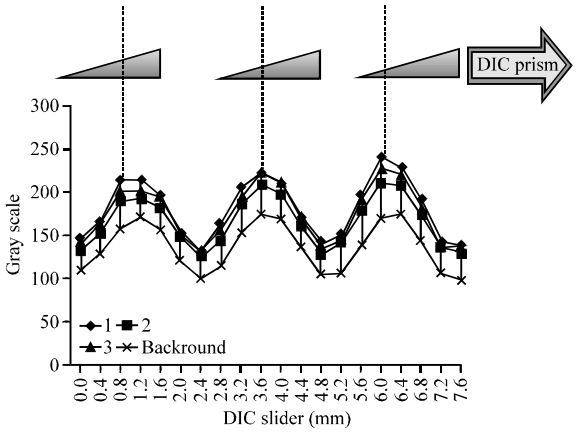

Fig. 9: Graph of maximum gray scale in Tap 1

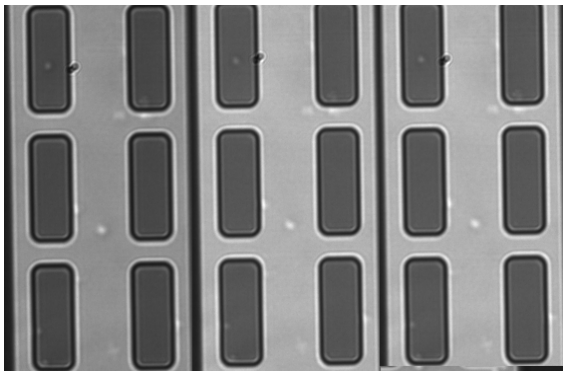

Fig. 10: Comparision before peak value and peak value (5.6/1.2/3.6 mm)

The gray scale graph shows peak values at 1.2, 3.6, 6.0 mm of DIC slider position and the peak value means the bright image. So, the brighter, the image looks better to the naked eye but in a qualitative aspect, it looks plain, not vivid. The more visual images appear before and after the peak value, rather than the peak value itself on the graph. When the slider positions are 5.6, 0.4, 2.8, 7.2 mm, the image is more apparent in that order and this result means the image is more vivid before the peak value than after the peak value. In Fig. 10, the image at the 5.6 mm before peak value is compared with 1.2 and 3.6 mm, peak values and the image difference to the naked eye is clear.

CONCLUSION

In this study, quantitative calibration of DIC for indentation mark verification in ACF image is investigated. Through the analysis of the indentation mark in ACF image experiment according to the DIC prism position, it comes out that there is a change in the gray

scale of indentation mark according to position change of the DIC slider and the change is periodic. In the result, the best image shows up before and after the peak value of the gray scale, not the peak value itself. In future, it is required to find a standard way to quantify the data and in the test of this study, 2-D camera is used which is not applied in the factory setting. Therefore for the practical purpose, the test with the line scan (1-D) camera which is included in factory setting is also required and the result should be analyzed and compared.

ACKNOWLEDGEMENT

This research (Grants No. C0268772) was supported by business for Academic-Industrial Cooperative Establishments funded Korea Small and Medium Business Administration in 2015. The researchers wish to thank Dae-Han Kim and Kean-Woo O who helped with the experiments.

REFERENCES

Dou, G., D.C. Whalley and C. Liu, 2008. Mechanical characterization of individual Ni-Au coated microsize polymer particles. Appl. Phys. Lett., 92: 104108-1-104108-3.

Erhardt, A., G. Zinser, D. Komitowski and J. Bille, 1985. Reconstructing 3-D light-microscopic images by digital image processing. Appl. Opt., 24: 194-200.

Kwon, W.S. and K.W. Paik, 2006. Experimental analysis of mechanical and electrical characteristics of metal-coated conductive spheres for Anisotropic Conductive Adhesives (ACAs) interconnection. IEEE. Trans. Compon. Packag. Technol., 29: 528-534.

Murphy, D.B. and M.W. Davidson, 2012. Differential Interference Contrast Microscopy and Modulation Contrast Microscopy. In: Fundamentals of Light Microscopy and Electronic Imaging, Murphy, D.B. and M.W. Davidson (Eds.). Wiley-Blackwell, Hoboken, New Jersey, pp: 173-197.

Watanabe, I., T. Fujinawa, M. Arifuku, K. Kobayashi and Y. Gotoh, 2004. Recent advances of interconnection technologies using anisotropic conductive films. Proceedings of the IEEE International Conference on Asian Green Electronics AGEC, January 7-9, 2004, IEEE, Japan isBN:0-7803-8203-X, pp: 229-234.

Yim, M.J., C.K. Chung and K.W. Paik, 2007. Effect of conductive particle properties on the reliability of anisotropic conductive film for chip-on-glass applications. IEEE. Trans. Electron. Packag. Manuf., 30: 306-312.

Yim, M.J., Y., Li, K.S. Moon, K.W. Paik and C.P. Wong, 2008. Review of recent advances in electrically conductive adhesive materials and technologies in electronic packaging. J. Adhes. Sci. Technol., 22: 1593-1630.